



Spatial heterogeneity and sources of soil carbon in southern African savannas

Lixin Wang^{a,c,*}, Gregory S. Okin^b, Kelly K. Caylor^c, Stephen A. Macko^{a,d}

^a Department of Environmental Sciences, University of Virginia, Charlottesville, VA 22904, United States

^b Department of Geography, 1255 Bunche Hall, University of California, Los Angeles, CA 90095, United States

^c Department of Civil and Environmental Engineering, Princeton University, Princeton, NJ, 08544, United States

^d Program in Geobiology and Low Temperature Geochemistry, US National Science Foundation, Arlington, VA 22230, United States

ARTICLE INFO

Article history:

Received 30 June 2008

Received in revised form 2 December 2008

Accepted 20 December 2008

Keywords:

Geostatistics

Kalahari

Savannas

Soil $\delta^{13}\text{C}$

Soil organic carbon

Stable isotope

ABSTRACT

Knowledge of the southern Africa soil carbon pool, its heterogeneity, sources (from trees or grasses), and potential response to climate is extremely limited. In this study the Kalahari Transect (KT) was used as a representative savanna ecosystem to quantitatively evaluate the spatial heterogeneity of the soil carbon pool and its contributing sources. The KT encompasses a dramatic aridity gradient on relatively homogenous soils. Two sites were chosen along the KT, representing dry and wet conditions. In February–March 2005, soil samples were collected at each site along a 300 m transect. Stable carbon isotope ($\delta^{13}\text{C}$) and organic carbon content (%C) of the soils were utilized in the assessment in conjunction with geostatistical analysis of the spatial patterns of soil $\delta^{13}\text{C}$ and %C. At the dry savanna site, well-defined patterns in both $\delta^{13}\text{C}$ and %C were observed that were related to the distribution of woody vegetation. At the wet savanna site, the spatial patterns of $\delta^{13}\text{C}$ and %C were somewhat less pronounced, but still were impacted by the distribution of woody vegetation. The relative contributions from C_3 and C_4 vegetation to the soil carbon pool at the wet site were independent of tree locations, but dependent on woody plant locations at the dry site. At the dry site, ~40% of the soil carbon was derived from C_3 vegetation, whereas at the wet site ~90% of the soil carbon originated from C_3 vegetation. These results represent an important step in understanding the impact of regional climate change (e.g., rainfall variations) on carbon sequestration in southern Africa by providing quantitative information on soil carbon spatial distributions and sources under different climatic conditions (e.g., different rainfall regimes).

© 2008 Elsevier B.V. All rights reserved.

1. Introduction

Soil organic matter (SOM) is one of the largest and most dynamic reservoirs of carbon (C) in the global C cycle. The amount of C stored in SOM is about twice that stored in the biosphere and atmosphere combined (Schlesinger, 1997). Africa is the second largest continent on Earth (20% of the Earth's land area), but knowledge of the soil C pool in Africa is extremely limited (Williams et al., 2007). The shared dominance of trees and grasses in savannas, the dominant physiognomy in southern Africa, and surface soil crust C fixation (e.g., Thomas et al., 2008), add more complexity in soil C pool partitioning and dynamics than is found in landscapes dominated by a single physiognomy. Previous work on regional C stack estimates have been treating trees and grasses as one vegetation pool without differentiating their contributions (Williams et al., 2007), which may limit our understand of the African C cycling since tree-grass composition is dynamic both spatially and temporally. By using stable C isotopes and soil organic carbon content in conjunction with geostatistical analysis,

this study aims to investigate the spatial variability of the soil C pool, partition the contributions of soil C from trees and grasses, and assess the variations in soil C spatial variability and sources under different climatic conditions.

The research was conducted at sites along the Kalahari Transect (KT), one of a set of IGBP (International Geosphere–Biosphere Programme) “megatransects” (Koch et al., 1995; Scholes et al., 2002) identified for global change studies. The soil substrate along the entire Transect is relatively homogenous, being covered by the Kalahari sands. The physical and hydraulic parameters such as soil texture (>96% of sand) and bulk density (around 1.4–1.5 g cm⁻³ along the whole Transect) do not have significant variations along the KT (Wang et al., 2007a). The KT thus provides an ideal setting to investigate changes in ecosystem dynamics, vegetation composition and structure, and C or nutrient cycles along a gradient of precipitation while minimizing confounding effects of soil heterogeneity.

As the two main plant functional types, the trees and grasses in African savannas differ in their photosynthetic pathways. Trees in this region utilize the C_3 photosynthetic pathway whereas grasses typically utilize the C_4 pathway (Caylor et al., 2005). Trees provide a browsing habitat for herbivores and provide fuel wood for human harvesting. Grasses are important fuel load for savanna fires therefore play a potential important role in regional climate due to the effect of

* Corresponding author. Department of Civil and Environmental Engineering, Princeton University, Princeton, NJ, 08544, United States. Tel.: +609 258 8308; fax: +609 258 1436.

E-mail address: lixinw@princeton.edu (L. Wang).

fire-produced aerosols on precipitation. The relative distribution of C_3 and C_4 vegetation along the KT has been extensively investigated in field (Ringrose et al., 1998; Scholes et al., 2002; Caylor, 2003; Privette et al., 2004; Scholes et al., 2004) and modeling studies (Jeltsch et al., 1998; Jeltsch et al., 1999; Caylor et al., 2004; Privette et al., 2004). However, the relative contributions of each vegetation type to the soil C pool and its variability under different climatic conditions are not well-understood. Because of the distinct $\delta^{13}C$ signatures for C_3 and C_4 plants (Farquhar et al., 1989), mixing models using $\delta^{13}C$ (C_3 vs. C_4) of plants and soil provide a unique tool to partition the soil C sources between C_3 and C_4 vegetation types. Carbon isotopes have been used to partition source carbon in many ecosystems (Balesdent et al., 1987; McPherson et al., 1993; Bond et al., 1994; Mariotti and Peterschmitt, 1994; West et al., 2000; Biggs et al., 2002). Although the SOM may undergo changes both spatially and temporally, the C isotope variations are not large enough to mask the difference between C_3 and C_4 plants (~14%). The average C isotopic values in the SOM and vegetation have been previously reported at sites along the KT (Bird et al., 2004; Swap et al., 2004; Wang et al., 2007a), though the spatial patterns at sites within this regional rainfall gradient, to our knowledge, have not been studied. In the present study, the spatial patterns in $\delta^{13}C$ and $\%C$ were explored at two sites along the KT that represent different climatic conditions (365 mm and 879 mm mean annual rainfall (MAP) respectively, dry and wet). The contributions of soil C from trees and grasses were partitioned to assess the variations in such contributions between the two climatic conditions. Three hypotheses were tested: 1) there are spatial patterns for soil $\delta^{13}C$ and $\%C$ at both ends of the KT (dry vs. wet); 2) the spatial pattern is better defined at the dry end of the Transect as we expect that precipitation-induced effects on the localized spatial pattern of vegetation

(i.e., more patchy vegetation at drier sites) would have corresponding effects on the localized spatial patterns of soil C and soil ^{13}C ; and 3) the contribution to soil C from C_3 and C_4 vegetations differs between wet and dry ends of the KT because of the different vegetation compositions at two ends.

2. Materials and methods

2.1. Field sites and field samplings

Two sites along the KT in Botswana with different climate conditions were chosen to compare the soil $\delta^{13}C$ and $\%C$ spatial patterns (Fig. 1). The present-day Kalahari climate ranges from arid to subhumid with relatively strong seasonal and interannual variations in precipitation. The MAP ranges from less than 200 mm in southwest Botswana to over 1000 mm in the north (i.e., western Zambia) (Shugart et al., 2004; Wang et al., 2007a). The two sites represent locations near the extremes for mean annual precipitation (MAP). Tshane is at the dry end of the Transect (~365 mm MAP) and Mongu is at the wet end of the Transect (~900 mm MAP). The vegetation in Mongu is woodland savanna dominated by tree species such as *Brachystegia spiciformis* Benth and the common grass species are *Eragrostis spp.* The vegetation in Tshane is open savanna dominated by *Acacia* species such as *A. luederitzii* Engl. and *A. mellifera* Benth, the dominant grass species are *Eragrostis lehmanniana* and *Schmidtia pappophoroides*. The above mentioned tree species are C_3 plants and the grass species are C_4 plants. A 300 m line transect oriented N–S was set up at each site. Surface soil samples (0–5 cm depth) were randomly collected along the 300 m transect using a soil auger: 271 samples were collected and analyzed from the Mongu (wet) site and 296

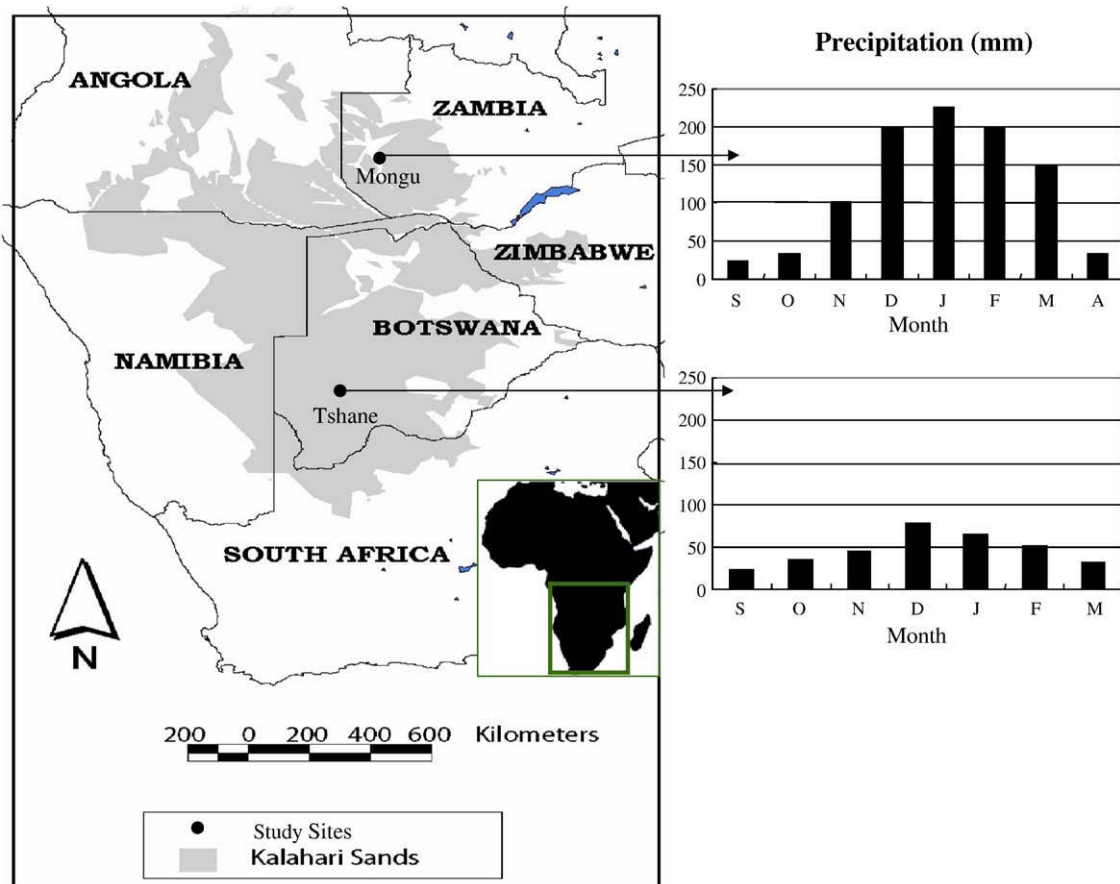


Fig. 1. Sampling locations and rainfall characteristics along the Kalahari Transect. The column charts are the mean annual monthly precipitation data (1961–1990) of the two sampling locations from Shugart et al. (2004).

samples were collected and analyzed from the Tshane (dry) site. The sampling locations were selected by the generation of random numbers prior to fieldwork. Irregular spacing of samples along the transect allowed us to have a large number of points that are closely spaced when calculating the variogram, while also allowing the transect to cover a relatively large distance. Such extensive soil samplings at each site (300 m transect) also likely captured the land use variations (if any) at each site. With the use of a transect, however, this sampling technique (compared to grid method) was not capable of identifying anisotropy in the distribution of soil nutrients of vegetation (Davis, 2002; Okin et al., 2008). Presence/absence of trees and shrubs (C_3 vegetation) at each sampling point was recorded. If C_3 vegetation is present, the soil is classified as under canopy soil, otherwise it is a between canopy soil.

2.2. Laboratory analysis

Soil samples collected for elemental and isotope analyses were oven dried at 60 °C in the laboratory, sieved to remove plant debris and homogenized using mortar and pestle. The presence of carbonates was tested by treating the soils with dilute hydrochloric acid (1 M) and no effervescence was observed. The %C was measured using an Elemental Analyzer (EA, Carlo Erba, NA1500, Italy) on the untreated soil samples. The stable C isotope analyses were performed using an Optima Isotope Ratio Mass Spectrometer (IRMS) connected to the EA (GV/Micromass, Manchester, UK). Stable isotope compositions are reported in the conventional form:

$$\delta^{13}C(\text{‰}) = \left[\left(\frac{^{13}C/^{12}C}{^{13}C/^{12}C}_{\text{standard}} \right) - 1 \right] \times 1000 \quad (1)$$

where $(^{13}C/^{12}C)_{\text{sample}}$ and $(^{13}C/^{12}C)_{\text{standard}}$ are the isotopic ratios of the sample and standard, respectively. The standard for C stable isotopes is Pee Dee Belemnite (PDB). Reproducibility of these measurements is typically better than 0.2‰ (Wang et al., 2007a).

2.3. Geostatistical analysis

Both conventional statistics and geostatistics were used to analyze the spatial features of the measured variables. Conventional statistics were used to indicate the degree of overall variation. Geostatistics were used to examine whether or not that variability is spatially structured.

Data normality for all data sets was tested (SAS 9.1, SAS Inc., Cary, NC, USA) before conventional statistical and geostatistical analyses. Data were log transformed when necessary to meet the normality requirement. Conventional statistics (i.e., mean, standard deviation and coefficient of variation (CV)) were calculated to indicate the overall variability for each analyzed item.

Geostatistical analysis was used to infer the spatial variation of soil $\delta^{13}C$ and %C at each site. Before semivariogram computation, the data were tested for 1st or 2nd order trends (Davis, 2002) using GS^+ software (Version 7.0, Gamma design software, Plainwell, MI, USA) and no trends were found.

A semivariogram (SV hereafter) is a plot of a series of semivariance values (γ) against the corresponding lag distances (h). The semivariance γ at each h is defined as:

$$\gamma(h) = \frac{1}{2N(h)} \sum_{i=1}^{N(h)} [z(i) - z(i+h)]^2 \quad (2)$$

where $N(h)$ is the number of sample pairs separated by the lag distance h . The $Z(i)$ is a measured value at location i and $Z(i+h)$ is a measured value at location $i+h$. There are several commonly used SV models. The model selection is based on two criteria: high R -square and fitted model shape. A spherical model was chosen to facilitate the comparison of

parameters between variables and because this model has been shown in many cases to be adequate for soil data (Schlesinger et al., 1996; Su et al., 2006; Wang et al., 2007b).

The spherical model is defined as:

$$\begin{aligned} \gamma(h) &= C_0 + C \left[1.5(h/A_0) - 0.5(h/A_0)^3 \right] \text{ for } h \leq A_0 \\ \gamma(h) &= C_0 + C \text{ for } h > A_0 \end{aligned} \quad (3)$$

where C_0 is nugget, A_0 is range and h is lag distance interval.

Three SV parameters were derived and used in the analysis: nugget (C_0), range (A_0) and the ratio of structure variance (C) and sill variance ($C+C_0$) ($C/(C+C_0)$), thereafter). Nugget reflects either the variability at scales finer than data resolution or variability due to measurement or locational error. Range indicates the distance of spatial autocorrelation between data pairs. The value $C/(C+C_0)$ is the proportion of the total variance that is spatially structured. A high $C/(C+C_0)$ indicates that variability in the dataset is strongly structured (Brooker, 1991; Li and Reynolds, 1995; Wang et al., 2007b).

The SVs were constructed using the jackknife method presented by Shafer and Varljen (1990) and discussed by Huisman et al. (2003) in a code written in the Interactive Data Language (IDL). All SVs were fit to the spherical model using a non-linear least squares fit employing the Levenberg–Marquardt algorithm, which combines the steepest descent and inverse-Hessian function fitting methods (Press et al., 1992). The uncertainties (95% confidence limits) were determined using the variance–covariance method of Pardo-Iguzquiza and Dowd (2001).

Because the sill of the semivariograms of $\delta^{13}C$ and %C at Tshane demonstrated periodicity, a hole effect model was also used to better fit these data following Ma and Jones (2001):

$$\gamma(h) = V[1 - \exp(-3h/A_0)\cos(bh)] \quad h \geq 0 \quad (4)$$

where V is the sill of the semivariogram plot, h is lag distance, A_0 is the effective range, $b=2\pi/\lambda$ is the angular frequency, and λ is the wavelength of the periodicity.

2.4. Soil C source partitioning

The main purpose of partitioning SOM according to the relative contribution from C_3 and C_4 plants is to assess the relative contribution of soil C from the two main plant functional types (trees vs. grasses) in a savanna ecosystem and the climatic dependence of such contributions. The soil C partitioning was calculated at each sampling point across the entire 300 m transect to reflect the overall variability in soil C partitioning at each site. The partition data were also combined with the tree/shrub presence data to assess how much of the C under canopy is from grass, how much of the C at between canopy area is from trees and how they vary across the two sites. At each sampling location, the $\delta^{13}C$ of C_3 and C_4 plants were used as two end-members in the two-source mixing ratio Eq. (5) to calculate the relative contributions of trees (f_{C3}) and grasses (f_{C4}) to soil C,

$$\delta^{13}C_{\text{SOM}} = \delta^{13}C_{C3} \times f_{C3} + \delta^{13}C_{C4} \times f_{C4} \quad (5)$$

where $\delta^{13}C_{\text{SOM}}$ is the $\delta^{13}C$ value of SOM (measured in this study), $\delta^{13}C_{C3}$ and $\delta^{13}C_{C4}$ are the $\delta^{13}C$ end-member values of C_3 and C_4 vegetation and f_{C3} and f_{C4} , which must sum to one, are relative contributions of trees and grasses to soil C. The end-member values of C_3 and C_4 vegetation were locally determined averages of root and foliar $\delta^{13}C$ of C_3 and C_4 plants at each site. The foliar $\delta^{13}C$ of C_3 and C_4 plants at each location were obtained during the 2005 wet season field campaign. The averages of 2–10 species (with 1–17 individuals for each species based on availability) for each plant functional type at each site were used to calculate foliar $\delta^{13}C$ of C_3 (–28.2‰ to –24.5‰ at Tshane and –30.6‰ to –25.7‰ at Mongu) and C_4 (–14.6‰ to –13.5‰ at Tshane and –14.5‰ to –12.8‰ at

Table 1
Summary of statistical parameters of soil $\delta^{13}\text{C}$ and %C at Tshane (dry) and Mongu (wet)

Location	Mean	SD	CV (%)	Min	Max	Skewness	
Tshane (Dry)	$\delta^{13}\text{C}$ (‰)	-17.2	3.5	-20.4	-25.1	-8.0	0.27
	%C	0.24	0.13	55.5	0.10	0.75	1.69
Mongu (Wet)	$\delta^{13}\text{C}$ (‰)	-24.9	1.0	-3.9	-27.1	-21.7	1.09
	%C	0.79	0.48	60.4	0.14	3.28	1.77

SD: Standard deviation.
CV: Coefficient of variation.

Table 2
Range (m) and proportion of structured variance $C/(C_0+C)$ for spherical models of variograms from both sites

Location	Analyte	Range (m)			$C/(C_0+C)$		
		M	L	U	M	L	U
Tshane (dry)	%C	9.08	8.96	9.20	0.96	0.92	1.00
	$\delta^{13}\text{C}$	9.66	9.42	9.90	0.62	0.58	0.66
Mongu (wet)	%C	4.77	4.59	4.95	0.64	0.59	0.68
	$\delta^{13}\text{C}$	5.04	4.59	5.49	0.48	0.44	0.52

M: the mean jackknife estimate.
L: the lower bound of the 95% confidence estimates.
U: the upper bound of the 95% confidence estimates.

Mongu) plants (Wang et al., 2009a). Five random individuals of both the C_3 (-26.6‰ to -23.3‰ at Tshane and -22.9‰ to -27.4‰ at Mongu) and C_4 (-13.5‰ to -12.4‰ at Tshane and -15.8‰ to -12.4‰ at Mongu) plants at each site were collected for the root $\delta^{13}\text{C}$ measurements (0–10 cm). The resulting $\delta^{13}\text{C}$ values of C_3 and C_4 end-members in Tshane were -25.4‰ and -13.6‰ respectively and the $\delta^{13}\text{C}$ values of C_3 and C_4

end-member in Mongu were -26.6‰ and -13.4‰ respectively. There is a clear difference in $\delta^{13}\text{C}$ between two photosynthetic pathways at both ends and such difference also overshadows the plant part $\delta^{13}\text{C}$ difference (e.g., foliar $\delta^{13}\text{C}$ vs. root $\delta^{13}\text{C}$) at each site.

3. Results and discussion

Soil $\delta^{13}\text{C}$ is higher at the Tshane (dry) site with mean value of -17.2‰, whereas the value at the Mongu (wet) site is -24.9‰ (Table 1). In contrast, the soil %C is higher at Mongu with mean value of 0.79%, compared to 0.24% at Tshane (Table 1). These results are in agreement with previous findings in this region (Hipondoka et al., 2003; Bird et al., 2004; Wang et al., 2007a). The smaller soil C pools at the drier site also agree with recent modeling results (Wang et al., 2009b). The coefficient of variation (CV) of soil $\delta^{13}\text{C}$ is much higher at Tshane (20.4%) compared to Mongu (3.9%) (Table 1). The CVs of soil %C are comparable at the two sites, with CV values of 55.5% and 60.4% at Tshane and Mongu respectively (Table 1).

There appear to be spatial patterns for both soil $\delta^{13}\text{C}$ and %C at both Tshane and Mongu but the range of autocorrelation is much larger at Tshane than at Mongu (Table 2; Fig. 2). At Tshane, the range of autocorrelation of soil $\delta^{13}\text{C}$ and %C is 9.66 m and 9.08 m, respectively (Fig. 2A; 2C). The excellent fit provided by the hole-effect model ($R^2=0.932$ and 0.928 for $\delta^{13}\text{C}$ and %C respectively) to the Tshane SVs underscores the strong spatial structuring of $\delta^{13}\text{C}$ and %C at this site (Fig. 2E; 2F). At Mongu, the range of autocorrelation of $\delta^{13}\text{C}$ and %C is 5.04 m and 4.77 m, respectively (Table 2; Fig. 2). The $C/(C+C_0)$ values for soil $\delta^{13}\text{C}$ are comparable between the two sites (Table 2; Fig. 2A and B) but the $C/(C+C_0)$ values for soil %C are much higher at Tshane (0.96) compared to

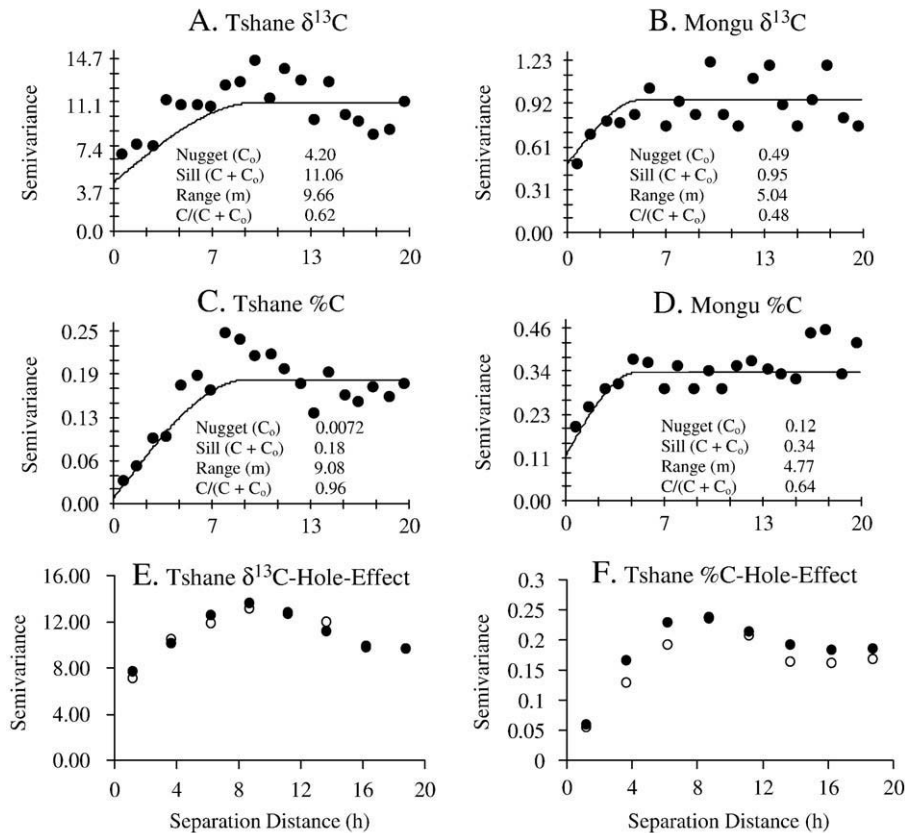


Fig. 2. Semivariograms of $\delta^{13}\text{C}$ at Tshane (A), Mongu (B), and semivariograms of %C at Tshane (C) and Mongu (D) along the Kalahari Transect using spherical models, and semivariograms of $\delta^{13}\text{C}$ (E) and %C (F) at Tshane using hole-effect model. For (E) and (F), the open circles are actual data points and the filled circles are the modeled data points, and the $R^2=0.932$ and 0.928 for (E) and (F) respectively. Under the curve is the summary of semivariogram spherical model parameters. Proportion structural variation $C/(C+C_0)$ is used as an index of the magnitude of spatial dependence.

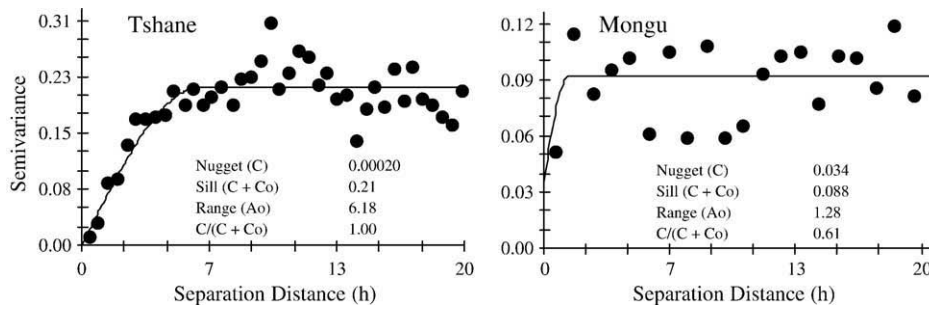


Fig. 3. Semivariograms of tree distributions at Tshane (A) and Mongu (B) along the Kalahari Transect using spherical models. Under the curve is the summary of semivariogram spherical model parameters. Proportion structural variation ($C/(C+C_0)$) is used as an index of the magnitude of spatial dependence.

Mongu (0.64) (Table 2; Fig. 2C; 2D). These results generally support the expectation that spatial patterns of soil $\delta^{13}\text{C}$ and $\%C$ would exist at both ends of the rainfall gradient and the spatial patterns would be stronger at the dry end, as denoted by higher values of $C/(C_0+C)$ at Tshane. The SVs of $\delta^{13}\text{C}$ and $\%C$ at Tshane showed a clear periodic pattern (Fig. 2A; 2C), which were successfully modeled using hole effect equation (Eq. (4)) with a wavelength (λ) of 18 m for both $\delta^{13}\text{C}$ and $\%C$ (Fig. 2E; 2F). The hole-effect behavior in Tshane also suggests a higher soil C heterogeneity at the dry end of the KT since hole-effect model generally represents the existence of multiple hierarchies in spatial patterns (Ma and Jones, 2001). The multiple hierarchies in soil C heterogeneity at the dry site are possibly caused by the aggregations of trees and shrubs at the dry site (Caylor et al., 2003).

There appear to be spatial patterns for tree distributions at both Tshane and Mongu but the range of autocorrelation is much larger at Tshane than at Mongu (Fig. 3). The range of autocorrelation of tree distribution at Tshane and Mongu is 6.2 m and 1.3 m, respectively (Fig. 3). The spatial distributions of soil C are strongly influenced by tree distributions at both ends of the Transect as indicated by two facts: 1) the range of autocorrelation of soil $\delta^{13}\text{C}$ and $\%C$ at both Tshane and Mongu are close to the mean woody-plant spacing distance at the corresponding locations ($\sim 6\text{--}10$ m at Tshane and $\sim 2\text{--}5$ m at Mongu, (Caylor, 2003; Okin et al., 2008); 2) the range of autocorrelation of soil $\delta^{13}\text{C}$ and $\%C$ at both Tshane and Mongu are close to the tree distribution autocorrelation range (Figs. 2 and 3). The canopy effects on soil $\delta^{13}\text{C}$ and $\%C$ distributions have also been found in other ecosystems such as bush encroached grassland in southwest US (Biggs et al., 2002).

There are significant differences in soil C partitions for under canopy and between canopy areas for both C_3 and C_4 vegetation in Tshane, but there are no differences in such partitions between “under canopy” and “between canopy” areas for both vegetation types in Mongu (Fig. 4). The results indicate that relative contributions from C_3 and C_4 vegetation to the soil C pool at the wet site is independent of tree locations, but dependent on woody plant locations at the dry site. Since leaf litter and root C are the major soil C sources and both field sites are generally flat, the independence in C distributions at wetter site is probably caused by the shorter mean woody-plant spacing distance and canopy rainfall interception can redistribute the leaf litter. At the dryer site, however, the wind confinement effect may over counter the rain redistribution effect. As a result, the tree leaf litters confine to under canopy areas and grass litters confine to grass canopy areas. The higher contributions from grasses at the between canopy areas at the drier site is likely due to the more extensive grass root distributions at surface, compared with trees (e.g., Wang et al., 2007a). The relative contribution of C_3 woody vegetation and C_4 grasses differs at the two sites. At the dry site, the grasses contributed the majority of soil C while only $\sim 40\%$ of the soil C is derived from woody C_3 vegetation. At the wet site, Mongu, the trees contributed the majority to soil C with $\sim 90\%$ of the soil C being derived from C_3 vegetation (Fig. 5). The variability in such contributions is much higher at the drier site, Tshane, than at Mongu (Fig. 5), providing further evidence that soil C heterogeneity is higher at the dry end of the KT. At both ends, there is a general linear trend between C_3 vegetation C contribution (fC_3) and soil $\%C$ ($R^2=0.2$ and 0.4 for Tshane and Mongu, respectively), indicating higher litter quality (low C/N) of trees to soil C

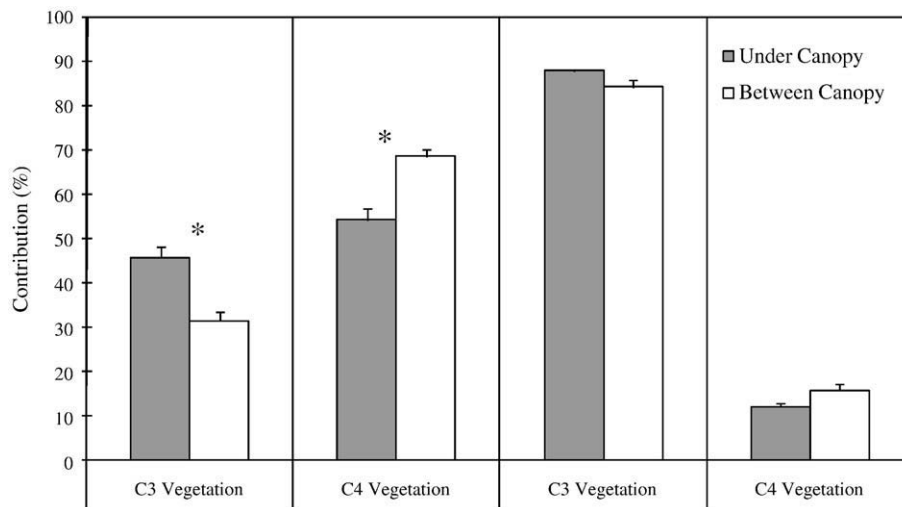


Fig. 4. The relative contributions to soil C from C_3 and C_4 vegetation for both under canopy (grey bar) and between canopy (white bar) areas at Tshane (left two panels) and Mongu (right two panels). The contribution differences between under and between canopy areas for each vegetation type at one particular location (e.g., C_3 vegetation contributions to soil C at under and between canopy areas at Tshane) were tested using Kuiper two-sample nonparametric test (due to the spatial correlations between the data points) and the significant differences at 0.05 significance level were indicated by asterisk.

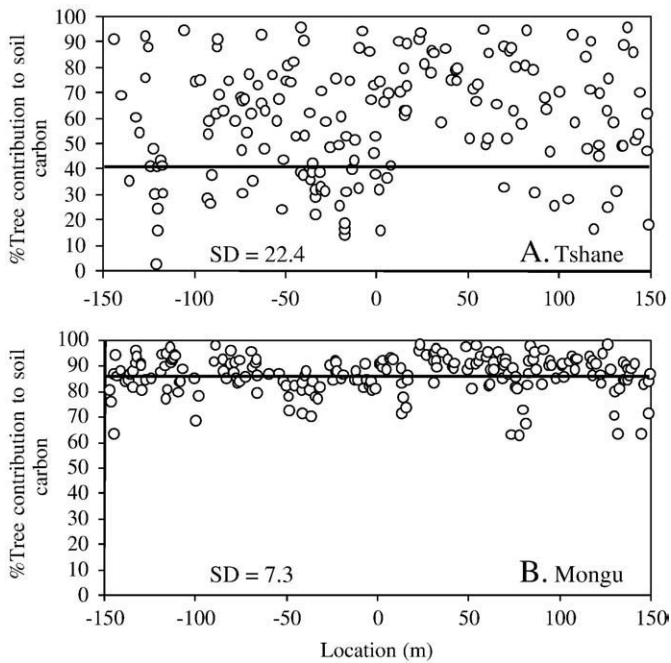


Fig. 5. The percentage of tree contributions to soil carbon at Tshane (A) and Mongu (B) along the entire 300 m transect using $\delta^{13}\text{C}$ mixing ratio calculations. The solid lines are the means of the contribution at each site. SD stands for standard deviation.

pools. These African savanna field sites are among the most pristine sites in the world without obvious human activity differences in the dry and wet ends. In addition, when selecting the site, we intended to choose locations with minimum apparent human activities. Since one of the major focuses of this study is to test the differences in soil C sources between “under canopy” and “between canopy” areas at each site, the human disturbance for these two types of environments, if any, should be able to canceled out considering a 300 m long transect at each site.

Due to the limited belowground information such as root density and root distribution, the SOM C source from vegetation in this study is calculated by averaging foliar and surface root (0–10 cm) $\delta^{13}\text{C}$ values as one end-member. Further studies of the weighted average of root $\delta^{13}\text{C}$ will be able to provide more accurate information on belowground C partition from C_3 and C_4 plants. In addition, considering root and foliar litter as separate end-members will better differentiate the SOM C source partition from aboveground and belowground litter input.

Field and modeling results, such as the co-kriging exercise, are vital for understanding the role of savannas in the terrestrial C budget. Recent analyses by Thomas et al. (2005) suggest that climate change may result in substantial drying in southern Africa, potentially resulting in the remobilization of sand dunes throughout the Kalahari. The realignment of vegetation associated with this regional drying suggests that there may be significant changes in soil C stocks in southern African savannas. In particular, the loss of woody vegetation associated with regional drying suggests, on the basis of this analysis, more heterogeneous and smaller soil C pools in the future since the Kalahari Transect itself can be interpreted as a chronosequence, where the drier sites may provide useful information on the long-term ecosystem responses to a decrease in MAP. Winothing associated with sand dune remobilization would also certainly result in the overall loss of soil C to the atmosphere. Thus, an important consequence of global climate change may be the reduction of the size of the soil C pool in southern African savannas, with excess C released to the atmosphere through soil respiration of organic C from remobilized sands. Understanding the size, patterns, and sources of soil organic C in savanna soils is a vital first step in determining the potential impact regional climate change on global C cycling.

4. Summary and Conclusions

Three hypotheses was tested in this study: 1) there are spatial patterns for soil organic C at both ends of the KT; 2) the spatial patterns are stronger at the dry end and 3) the contributions to soil C from C_3 and C_4 vegetations differ between wet and dry ends. Geostatistical analyses of $\delta^{13}\text{C}$ and %C and isotope partitioning of soil C source in surface soils support all three of these hypotheses. In particular, the results suggest that the distribution of woody vegetation is a major determinant of the size and spatial structure of the soil C pool as well as the spatial structure of C isotopic composition. The results also suggest that the contribution of C_4 vegetation to the C pool of surface soils is greater in drier savannas compared to wet savannas, a consequence of the greater grass productivity at the drier sites. Although there are grasses in at the wet end of the KT, they do not appear to contribute significantly to the surface C pool.

These results indicate that in structurally complex savanna ecosystems, accurate estimates of C storage must take into account both patterns of soil C (i.e., soil C distributions) as well as the sources and processes that contribute to the soil C pool (i.e., decomposition, soil C sequestration and soil respiration). We further find that there is a close relationship between the patterns of soil organic C and the process that give rise to these patterns. Specifically, a heterogeneous woody structure is largely responsible for the heterogeneity in both the source and amount of organic C in the surface soils. This relationship suggests that high-resolution remote sensing techniques that can identify and characterize the spatial distribution of woody vegetation (Scanlon and Albertson, 2003; McGlynn and Okin, 2006; Wang et al., 2009c) may be able to contribute substantively to the estimation of C stocks in savannas. For instance, covariance between soil organic C concentrations and isotopic compositions documented here may be able to be used in a co-kriging approach to estimate C reservoir and isotopic compositions on a regional scale.

Acknowledgements

The project was supported by NASA-IDS2 (NNG-04-GM71G). We greatly appreciate the team-work and field assistance from Paolo D’Odorico, Natalie Mladenov, Matt Therrell (University of Virginia), and Billy Mogojuw, Dikitso Kolokose, O.G.S.O. Kgosidintsi and Thoralf Meyer (University of Botswana) as well as Kebonyethata Dintwe (Department of Agriculture, Botswana). We thank two anonymous reviewers for their thoughtful comments. This manuscript is based in part on IR/D support by the National Science Foundation, to SAM while working at the Foundation. Any opinion, finding, and conclusions or recommendations expressed in this material are those of the authors and do not necessarily reflect the views of the National Science Foundation.

References

- Balesdent, J., Mariotti, A., Guillet, B., 1987. Natural ^{13}C abundances as a tracer for studies of soil organic matter dynamics. *Soil Biology & Biochemistry* 19, 25–30.
- Biggs, T.H., Quade, J., Webb, R.H., 2002. $\delta^{13}\text{C}$ values of soil organic matter in semiarid grassland with mesquite (*Prosopis*) encroachment in southeastern Arizona. *Geoderma* 110, 109–130.
- Bird, M.I., Veenendaal, E.M., Lloyd, J.J., 2004. Soil carbon inventories and d^{13}C along a moisture gradient in Botswana. *Global Change Biology* 10 (3), 342–349.
- Bond, W.J., Stock, W.D., Hoffman, M.T., 1994. Has the Karoo spread? A test for desertification using carbon isotopes from soils. *South African Journal of Science* 90, 391–397.
- Brooker, P.I., 1991. A geostatistical primer. World Scientific Publishing Co. Pte. Ltd, Singapore.
- Caylor, K.K., 2003. The structure and function of Kalahari transect vegetation. PhD dissertation.
- Caylor, K.K., Dowty, P.R., Shugart, H.H., Ringrose, S., 2004. Relationship between small-scale structural variability and simulated vegetation productivity across a regional moisture gradient in southern Africa. *Global Change Biology* 10 (3), 374–382.
- Caylor, K.K., Shugart, H.H., Dowty, P.R., Smith, T.M., 2003. Tree spacing along the Kalahari transect in southern Africa. *Journal of Arid Environments* 54, 281–296.
- Caylor, K.K., Shugart, H.H., Rodriguez-Iturbe, I., 2005. Tree canopy effects on simulated water stress in southern African savannas. *Ecosystems* 8 (1), 17–32.
- Davis, J.C., 2002. Statistics and data analysis in geology. John Wiley & Sons, New York.
- Farquhar, G., Ehleringer, J., Hubick, K., 1989. Carbon isotope discrimination and photosynthesis. *Annual Review of Plant Physiology and Molecular Biology* 40, 503–537.

- Hipondoka, M.H.T., Aranibar, J.N., Chirara, C., Lihavha, M., Macko, S.A., 2003. Vertical distribution of grass and tree roots in arid ecosystems of Southern Africa: niche differentiation or competition. *Journal of Arid Environments* 54, 319–325.
- Huisman, J.A., Snepvangers, J.J.J.C., Bouten, W., Heuvelink, G.B.M., 2003. Monitoring temporal development of spatial soil water content variation: comparison of ground penetrating radar and time domain reflectometry. *Vadose Zone Journal* 2, 519–529.
- Jeltsch, F., Moloney, K., Milton, S.J., 1999. Detecting process from snapshot pattern: lessons from tree spacing in the southern Kalahari. *Oikos* 85, 451–466.
- Jeltsch, F., Milton, S.J., Dean, W.R.J., Rooyen, N.V., Moloney, K.A., 1998. Modelling the impact of small-scale heterogeneities on tree-grass coexistence in semi-arid savannas. *Journal of Ecology* 86, 780–793.
- Koch, G.W., Scholes, R.J., Steffen, W.L., Vitousek, P.M., Walker, B.H., 1995. The IGBP terrestrial transects: Science plan, Report No. 36. International Geosphere–Biosphere Programme, Stockholm.
- Li, H.R., Reynolds, J.F., 1995. On the quantification of spatial heterogeneity. *Oikos* 73, 280–284.
- Ma, Y.Z., Jones, T.A., 2001. Teacher's aide: modeling hole-effect variograms of lithology-indicator variables. *Mathematical Geology* 33 (5), 631–648.
- Mariotti, A., Peterschmitt, E., 1994. Forest savanna ecotone dynamics in India as revealed by carbon isotope ratios of soil organic matter. *Oecologia* 97, 475–480.
- McGlynn, I.O., Okin, G.S., 2006. Characterization of shrub distribution using high spatial resolution remote sensing: ecosystem implication for a former Chihuahuan Desert grassland. *Remote Sensing of Environment* 101 (4), 554–566.
- McPherson, G.R., Boutton, T.W., Midwood, A.J., 1993. Stable carbon isotope analysis of soil organic matter illustrates vegetation change at the grassland/woodland boundary in southeastern Arizona, USA. *Oecologia* 93, 95–101.
- Okin, G.S., Mladenov, N., Wang, L., Cassel, D., Caylor, K.K., Ringrose, S., Macko, S., 2008. Spatial patterns of soil nutrients in two southern African savannas. *Journal of Geophysical Research* 113, G02011.
- Pardo-Iguzquiza, E., Dowd, P., 2001. Variance-covariance matrix of the experimental variogram: assessing variogram uncertainty. *Mathematical Geology* 33 (4), 397–419.
- Press, W.H., Teukolsky, S.A., Vetterling, W.T., Flannery, B.P., 1992. *Numerical recipes in C: the art of scientific computing*. Cambridge University Press, Cambridge.
- Privette, J.L., Tian, Y., Roberts, G., Scholes, R.J., Wang, Y., Caylor, K.K., Frost, P., Mukelabai, M., 2004. Vegetation structure characteristics and relationships of Kalahari woodlands and savannas. *Global Change Biology* 10, 281–291.
- Ringrose, S., Matheson, W., Vanderpost, C., 1998. Analysis of soil organic carbon and vegetation cover trends along the Botswana Kalahari Transect. *Journal of Arid Environments* 38, 379–396.
- Scanlon, T.M., Albertson, J.D., 2003. Inferred controls on tree/grass composition in a savanna ecosystem: combining 16-Year NDVI data with a dynamic soil moisture model. *Water Resource Research* 39 (8), 1224. doi:10.1029/2002WR001881.
- Schlesinger, W.H., 1997. *Biogeochemistry: an analysis of global change*. Academic Press, New York.
- Schlesinger, W.H., Raikes, J.A., Hartley, A.E., Cross, A.F., 1996. On the spatial pattern of soil nutrients in desert ecosystems. *Ecology* 77 (2), 364–374.
- Scholes, R.J., Frost, P.G.H., Tian, Y., 2004. Canopy structure in savannas along a moisture gradient on Kalahari sands. *Global Change Biology* 10 (3), 292–302.
- Scholes, R.J., Dowty, P.R., Caylor, K., Parsons, D.A.B., Frost, P.G.H., Shugart, H.H., 2002. Trends in savanna structure and composition along an aridity gradient in the Kalahari. *Journal of Vegetation Science* 13, 419–428.
- Shafer, J.M., Varlijen, M.D., 1990. Approximation of confidence-limits on sample semi-variograms from single realizations of spatially correlated random-fields. *Water Resources Research* 26 (8), 1787–1802.
- Shugart, H.H., Macko, S.A., Lesolle, P., Szuba, T.A., Mukelabai, M.M., Dowty, P., Swap, R.J., 2004. The SAFARI 2000-Kalahari Transect wet season campaign of year 2000. *Global Change Biology* 10, 273–280.
- Su, Y., Li, Y., Zhao, H., 2006. Soil properties and their spatial pattern in a degraded sandy grassland under post-grazing restoration, Inner Mongolia, northern China. *Biogeochemistry* 79 (3), 297–314.
- Swap, R.J., Aranibar, J.N., Dowty, P.R., Gilhooly, W.P., Macko, S.A., 2004. Natural abundance of ^{13}C and ^{15}N in C_3 and C_4 vegetation of southern Africa: patterns and implications. *Global Change Biology* 10 (3), 350–358.
- Thomas, A.D., Hoon, S.R., Linton, P.E., 2008. Carbon dioxide fluxes from cyanobacteria crusted soils in the Kalahari. *Applied Soil Ecology* 39, 254–263.
- Thomas, D.S.G., Knight, M., Wiggs, G.F.S., 2005. Remobilization of southern African desert dune systems by twenty-first century global warming. *Nature* 435, 1218–1221.
- Wang, L., D'Odorico, P., Ringrose, S., Coetzee, S., Macko, S., 2007a. Biogeochemistry of Kalahari sands. *Journal of Arid Environments* 71 (3), 259–279. doi:10.1016/j.jaridenv.2007.03.016.
- Wang, L., Mou, P.P., Huang, J., Wang, J., 2007b. Spatial variation of nitrogen availability in a subtropical evergreen broadleaved forest of southwestern China. *Plant and Soil* 295, 137–150. doi:10.1007/s11104-007-9271-z.
- Wang, L., D'Odorico, P., Ries, L., Macko, S., 2009a. Patterns and implications of plant-soil $\delta^{13}\text{C}$ and $\delta^{15}\text{N}$ values in African savanna ecosystems. *Quaternary Research*. doi:10.1016/j.yqres.2008.11.004.
- Wang, L., D'Odorico, P., Manzoni, S., Porporato, A., Macko, S., 2009b. Carbon and nitrogen dynamics in southern African savannas: the effect of vegetation-induced patch-scale heterogeneities and large scale rainfall gradients. *Climatic Change*. doi:10.1007/s10584-009-9548-8.
- Wang, L., Okin, G.S., Macko, S., 2009c. Satellite prediction of soil $\delta^{13}\text{C}$ distributions in a southern African savanna. *Journal of Geochemical Exploration*. doi:10.1016/j.gexplo.2008.10.003.
- West, A.G., Bond, W.J., Midgley, J.J., 2000. Soil carbon isotopes reveal ancient grassland under forest in Hluhluwe, KwaZulu-Natal. *South African Journal of Science* 96, 252–254.
- Williams, C.A., Hanan, N.P., Neff, J.C., Scholes, R.J., Berry, J.A., Denning, A.S., Baker, D.F., 2007. Africa and the global carbon cycle. *Carbon Balance and Management* 2, 3. doi:10.1186/1750-0680-2-3.